



OPEN

Sectional measurements of shoulder muscle volume and computed tomography density in anterior shoulder instability

Keita Nagawa¹✉, Yuki Hara¹, Hirokazu Shimizu¹, Koichiro Matsuura¹, Kaiji Inoue¹, Eito Kozawa¹, Katsunobu Sakaguchi² & Mamoru Niitsu¹

In patients with anterior shoulder instability (ASI), a chronic imbalance might exist between the anterior and posterior shoulder muscles (i.e., subscapular [Ssc] vs. infraspinatus and teres minor [Isp + TM]). The balance could be evaluated as the ratio of volume (VR_{Ssc/Isp+TM}) and computed tomography density (CT-DR_{Ssc/Isp+TM}) using a 3D sectional approach. A total of 28 CT images (19 patients) of non-pathological shoulders (clavicular fracture [CF]) and 17 CT images (17 patients) of ASI were used. Segmentation of Ssc and Isp + TM muscles was performed; the reconstructed models were separated by the Y-view plane and the planes situated 2.5 cm and 5 cm medial to the Y-view plane to generate muscle models. VR_{Ssc/Isp+TM} and CT-DR_{Ssc/Isp+TM} were measured in each section of both the groups, as well as in whole muscle measurements in the CF group. VR_{Ssc/Isp+TM} and CT-DR_{Ssc/Isp+TM} obtained through a 3D sectional approach in the CF group were comparable to the whole muscle measurements, with a value of 1.06 for both. In the ASI group, the VR_{Ssc/Isp+TM} was higher, whereas the CT-DR_{Ssc/Isp+TM} was lower than those in the CF group. The VR_{Ssc/Isp+TM} and CT-DR_{Ssc/Isp+TM} appeared to be balanced in the CF group. However an imbalance was observed in the ASI group. Our 3D sectional measurement approach has the potential to assess the balance between the anterior and posterior shoulder muscles in ASI.

Anterior shoulder instability (ASI), also called recurrent anterior shoulder dislocation, is a common problem in young athletic individuals^{1,2}. ASI is a pathological condition in which the humeral head subluxes or dislocates from the glenoid fossa due to a soft-tissue or bone injury, causing shoulder joint symptoms and reducing function. Repeated dislocations damage the static structures involved in joint support, such as the labrum, capsule, ligaments, and bone, which further increases instability¹. Bankart injury and Hill–Sachs deformity are well-known lesions related to ASI. The treatment of ASI has evolved owing to the advances in arthroscopic techniques, along with an improved understanding of the shoulder anatomy and its complex biomechanics^{3,4}.

In the shoulder joint area, the degree of muscle atrophy and fatty degeneration of the muscles that make up the shoulder joint are often investigated as factors that indicate the functional prognosis after surgery. These parameters are highly versatile indicators of postoperative muscle strength and joint stability. Many studies have been conducted on rotator cuff repair after shoulder rotator cuff tears, which have shown the utility of specific parameters, such as the cross-sectional area and occupancy of shoulder muscles in oblique sagittal images, called the Y-view, tangent sign, and Goutallier classification^{5–7}.

The rotator cuff muscles are dynamic stabilizers of the shoulder joint but not primarily involved in shoulder instability compared to static structures. Therefore, few reports have investigated shoulder muscle atrophy and fatty degeneration in cases of ASI. In a recent report by Mitterer et al.⁸, a muscle volume analysis was performed in patients with posterior humeral head subluxation. They observed a significant volume imbalance in the transverse force couple of the shoulder muscle (subscapularis [Ssc] vs. infraspinatus and teres minor muscle [Isp + TM]) in those patients, indicating an unbalanced anterior-posterior muscle force that may contribute to shoulder joint instability. In previous studies, the volume ratio between Ssc and Isp + TM (VR_{Ssc/Isp+TM}) was observed to be 1.02 ± 0.18 in healthy participants, regardless of age or sex⁹. In the aforementioned report, this ratio was 1.14 ± 0.13 for patients with posterior humeral head subluxation⁸, which was higher than that for healthy participants. The computed tomography (CT) density ratio between Ssc and Isp + TM (CT-DR_{Ssc/Isp+TM})

¹Department of Radiology, Saitama Medical University, 38 Morohongou, Moroyama-machi, Iruma-gun, Saitama, Japan. ²Department of Orthopedics, Saitama Medical University, 38 Morohongou, Moroyama-machi, Iruma-gun, Saitama, Japan. ✉email: Ideso5rbldayids9taiy@gmail.com

could also be a useful indicator for the assessment of fatty degeneration of muscles. However, to the best of our knowledge, no study has examined this ratio in patients with ASI.

In fact, the mechanism of shoulder joint instability is more complicated, and a recent concept of multidirectional shoulder instability has been introduced that involves dislocation in multiple directions, rather than a simple anterior-posterior dislocation^{10,11}. Therefore, research investigating VR_{Ssc/Isp+TM} and CT-DR_{Ssc/Isp+TM} in patients with shoulder instability may provide a new perspective on the instability factors of the shoulder joint; however, studies on this topic are scarce. One of the reasons is that on CT or MRI, the shoulder muscles are often imaged partially in cases of ASI because they are not points of priority in the evaluation compared to the bone, labrum, and cartilage. To accurately assess these ratios, the entire muscle area should ideally be examined; in cases where partial assessment is unavoidable, determining the extent to which the ratio obtained from the partial muscle volume reflects the overall ratio should be a prerequisite.

In the present study, we hypothesized that a CT-based sectional (partially cut) measurement approach has the potential to assess imbalance between the anterior and posterior muscle force in ASI. Therefore, our objectives were to (1) verify whether VR_{Ssc/Isp+TM} and CT-DR_{Ssc/Isp+TM} obtained by three-dimensional (3D) sectional muscle measurements could be substitutes for those obtained from the whole muscle using the CT data of non-pathologic shoulders (patients with clavicular fracture [CF]); and (2) examine VR_{Ssc/Isp+TM} and CT-DR_{Ssc/Isp+TM} in cases of ASI and assess the difference between ASI and non-pathologic shoulders by comparing the two experiments.

Methods

Experimental procedure

Step A

CT data of non-pathologic shoulders (patients with CF) were collected. In each image, the segmentation of Ssc and Isp+TM was performed. Subsequently, we obtained the VR_{Ssc/Isp+TM} and CT-DR_{Ssc/Isp+TM} using sectional or whole-muscle measurements. By comparing these results, we evaluated whether sectoral muscle evaluation was an effective technique.

Step B

Shoulder CT data were collected from patients with ASI. The segmentation and measurement of the muscles were performed in the same manner as in step A, except that they were all evaluated through sectional muscle measurement (as part of the muscle was always out of range in our protocol). We then assessed the differences between the ASI and CF groups by comparing the results of steps A and B.

Participants

This study was approved by the Research Ethics Committee of the Saitama Medical University Hospital (approval number 2022-072). All experiments were performed in accordance with the relevant guidelines and regulations. The requirement of this study for informed consent was waived by the Research Ethics Committee of Saitama Medical University Hospital.

Step A (CF group)

Patients with CF who underwent shoulder CT before surgery at our institution between January 2012 and December 2021, with an order from the Department of Orthopedics at our hospital, were identified and reviewed. Figure 1A presents the inclusion and exclusion criteria of this study. A total of 28 CT data from 19 patients were analyzed.

Step B (ASI group)

Patients diagnosed with ASI who underwent shoulder CT before arthroscopic surgery at our institution between January 2012 and December 2021, with an order from the Department of Orthopedics at our hospital, were identified and reviewed. Figure 1B presents the inclusion and exclusion criteria of this study. A total of 17 CT images from 17 patients were analyzed.

The preoperative clinical and demographic status of patients with ASI (Step B) was determined as follows: symptom duration, number of symptomatic dislocations, sports activity/work level, and preoperative range of motion. Additionally, preoperative morphological findings such as glenoid rim morphology, Hill-Sachs lesion, anterior inferior glenohumeral ligament hyperlaxity, and capsule tears were demonstrated. Glenoid rim morphology and Hill-Sachs lesion was determined as described by Nakagawa et al.¹². Glenoid rim morphology was classified into erosion and fragment types, while glenoid defect size was designated as “large” if it exceeded 15 mm and “small” if less than 15 mm. Hill-Sachs lesion length and width were measured on 3D CT reconstructed images and designated as “large” (width > 15 mm or length > 30 mm) or small (width < 15 mm or length < 30 mm). Anterior inferior glenohumeral ligament hyperlaxity and capsule tears were determined by arthroscopy.

CT acquisition

CT was performed using a 128-multislice CT Siemens SOMATOM Definition Flash scanner (Siemens Healthcare, Erlangen, Germany). Patients were examined while in a supine position lying on their abdomen with their arms adducted and hands in a neutral position. CT was performed using the standard dedicated CT protocol for the shoulders used at our institution. The slice thickness was 2 mm with reformations in the axial, coronal, and sagittal planes. The field of view was 25 × 25 × 15 cm and 15 × 15 × 9 cm in step A and step B, respectively.

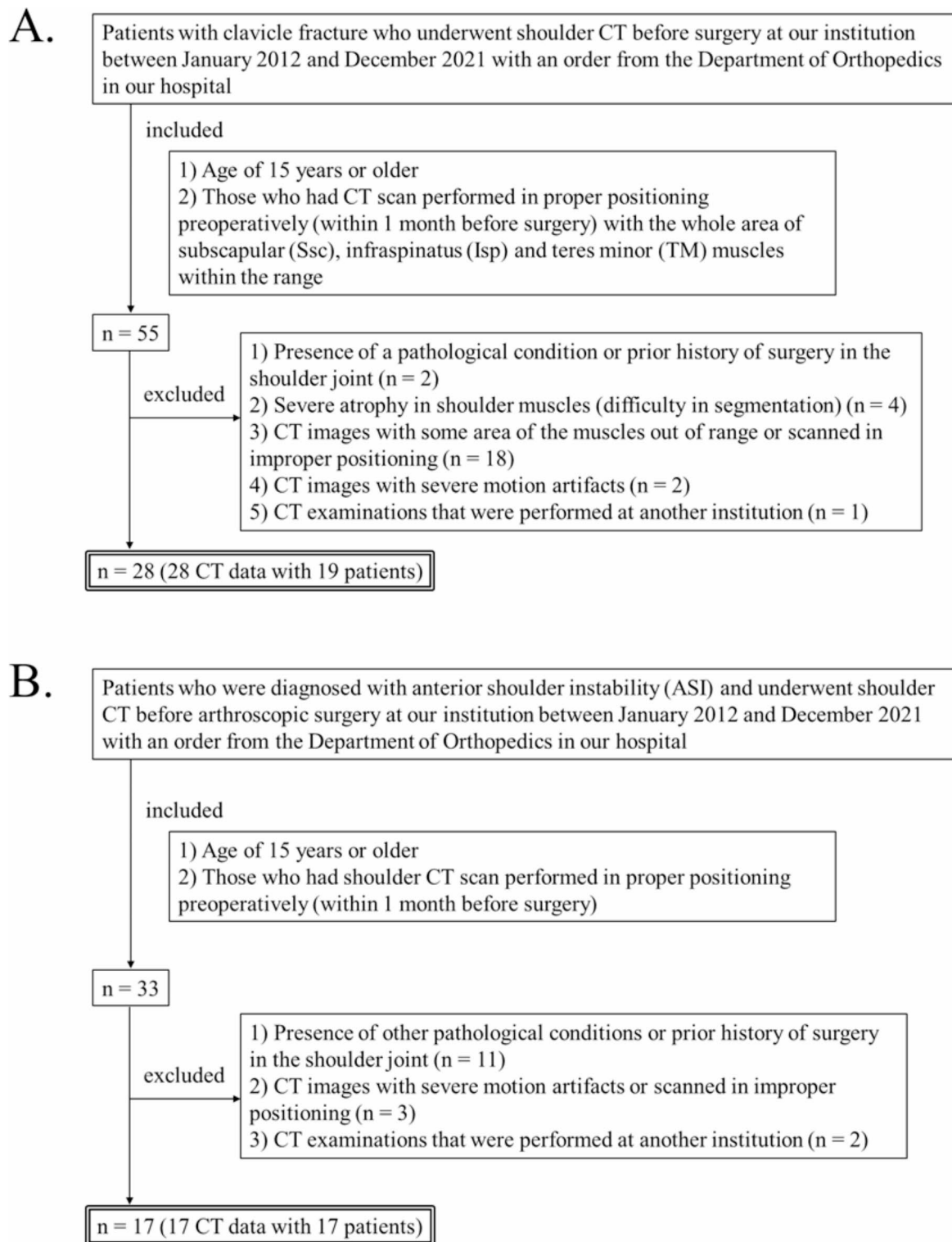


Fig. 1. Flow chart of the inclusion and exclusion criteria for the study.

Measurement of the volume and CT density of the shoulder muscles

To measure the volume and CT density of the shoulder muscles, we employed the method described by Mitterer et al.⁸ Segmentation was performed using an open-source software (ITK-SNAP veASion 3.8.0). After the CT scans were loaded into ITK-SNAP using the Digital Imaging and Communications in Medicine format, the Ssc and Isp + TM areas were delineated on every transverse slice using semi-automatic segmentation tools (Fig. 2A). From the delineated contour, a 3D model of each shoulder muscle was reconstructed and saved as a standard 3D model in the NIFTI file format (*.nii.gz).

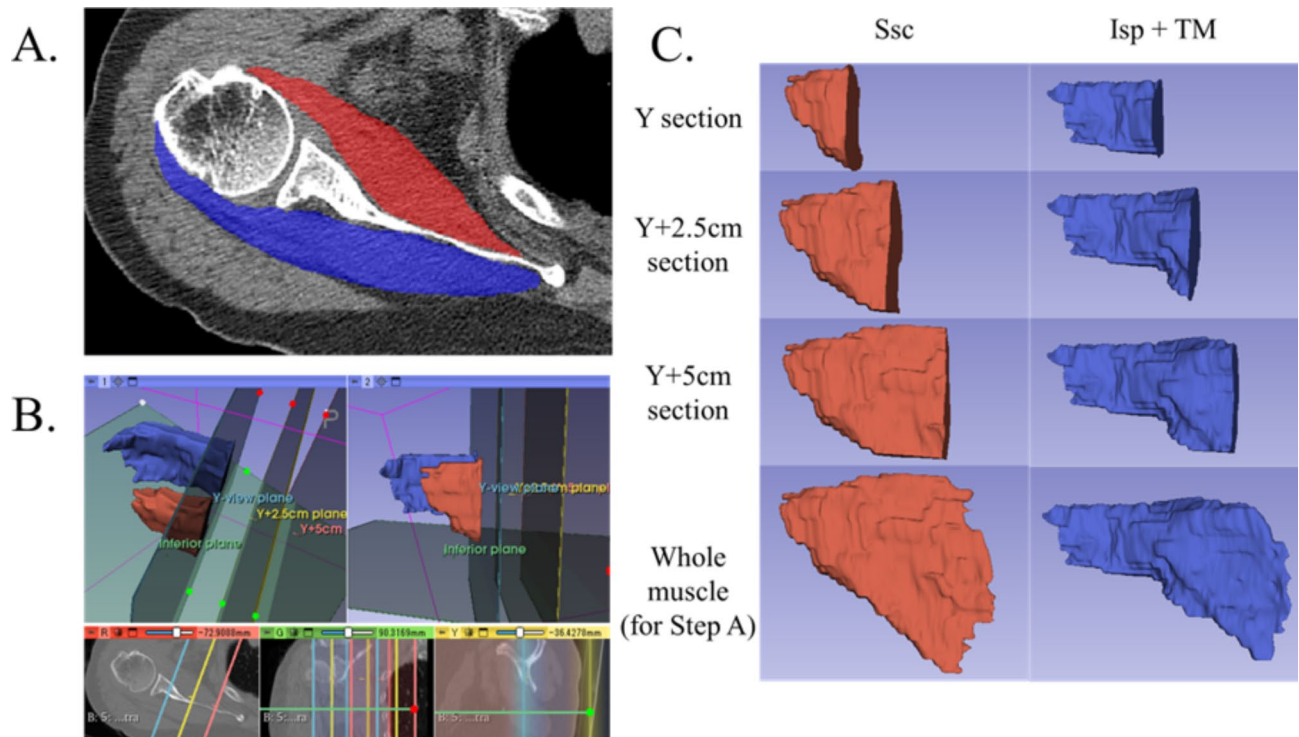


Fig. 2. (A) The areas of subscapular muscle (Ssc, red) and infraspinatus and teres minor muscles (Isp + TM, blue) in every axial image are delineated by applying semi-automatic segmentation tools. (B) The 3D models of Ssc and Isp + TM are separated by the Y-view plane (blue), Y + 2.5 cm plane (yellow), and Y + 5 cm plane (red) using the Dynamic Modeler module. Moreover, we implemented a cut off at the plane 3 cm inferior to the lower end of the glenoid labrum (green) to exclude the inferior margin of each muscle volume, because this area was usually out of range in our shoulder CT protocol. (C) For each 3D model of Ssc and Isp + TM muscles, three sections of 3D models were newly created (hence, we obtained six sectional muscle models): from the most lateral end of the muscles to the plane of Y-view (Y section), to the plane 2.5 cm medial to the Y-view (Y + 2.5 cm section), and to the plane 5 cm medial to the Y-view (Y + 5 cm section). For step A, we performed the whole muscle measurement as well.

To perform a 3D sectional (i.e., cut by cross-sections) muscle assessment, the technique proposed by Chung et al. was adopted¹³. We performed sectional measurements of the shoulder muscles at the following three specific planes: from the most lateral end of the muscles to the plane of the Y-view (Y section), to the plane 2.5 cm medial to the Y-view (Y + 2.5 cm section), and to the plane 5 cm medial to the Y-view (Y + 5 cm section). Additionally, we implemented a cut off at the plane 3 cm inferior to the lower end of the glenoid labrum to exclude the inferior margin of each muscle volume, as this area was usually out of range in our shoulder CT protocol (Fig. 2B). By implementing these adjustments, we created sectional muscle models and determined their volumes and CT densities. The mean CT density (i.e. mean scalar value) was calculated from the binary label map representation of the segmented muscle regions that overlap with the selected scalar volume. In step A, the whole muscle volume and CT density were calculated (Fig. 2C). Finally, we obtained the ratio of muscle volume to CT density between the Ssc and Isp + TM ($VR_{Ssc/Isp+TM}$ and $CT-DR_{Ssc/Isp+TM}$) for each section. All procedures were conducted using an open-source software (3D Slicer 5.0.3), and the specific implementation schemes are detailed in the Supplementary Information.

Associations between the ratios obtained from each sectional measurement were evaluated using Pearson's correlation coefficient and a paired t-test. To assess interobserver reproducibility in the segmentation and measurement process, two radiologists with 7 and 6 years of experience performed these steps independently. Both radiologists were blinded to the clinical information. The intraclass correlation coefficient (ICC) was measured to evaluate interobserver reproducibility.

Comparison and post hoc power analysis of step A and step B results

To compare the CF (Step A) and ASI (Step B) patients, the results of the sectional muscle volume, CT density, and ratios therein were statistically compared using an unpaired Student's t-test. Furthermore, to determine the study's ability to detect a significant effect, a post hoc power analysis was performed for each item of the comparison. The Cohen's d value required to quantify the effect size was calculated as follows:

$$s = \sqrt{\frac{(n_1 - 1) \times s_1 + (n_2 - 1) \times s_2}{n_1 + n_2 - 2}}$$

where s is the pooled standard deviation, n_1 and n_2 are the sizes of the first and second samples, and s_1 and s_2 is the variance of the first and second samples.

$$d = \frac{u_1 - u_2}{s}$$

where d is the Cohen's d value, u_1 is the mean of the first sample, u_2 is the mean of the second sample, and s is the pooled standard deviation of both samples.

Finally, the estimated required sample size was calculated by a statistical power analysis using an unpaired Student t-test. The parameters for the analysis were set as follows: significance level (alpha value), 0.05; minimal statistical power (effect size), 0.80; and statistical power, 0.80. The expected ratio of the sample sizes from one sample to the other was set at 1.0.

Statistical analyses were performed using the open-source software package (Python scikit-learn 0.22.1). Statistical significance was set at $p < 0.05$.

Results

Step A

A total of 28 CT images from 19 patients (including both sides of the shoulders in nine patients) were included in this study. The mean age \pm standard deviation was 56.7 ± 9.9 years. The sex ratio was 13/6 (male/female). The side scanned on CT was 14/14 (right/left). The CF side measures 7/12 (right/left). Interobserver reproducibility was good for all 3D volumes, with a mean ICC value of 0.821.

The observed ratios of the muscle volume (VR $_{Ssc/Isp+TM}$) for Y, Y + 2.5 and Y + 5 sections and for the entire muscle were 1.09 ± 0.27 , 1.09 ± 0.17 , 1.06 ± 0.16 , and 1.06 ± 0.10 , respectively. A moderate correlation was observed between the VR $_{Ssc/Isp+TM}$ of the Y + 2.5 section and the entire muscle volume ($r = 0.651$).

The observed ratios of CT density (CT-DR $_{Ssc/Isp+TM}$) for Y, Y + 2.5 and Y + 5 sections and for the entire muscle were 1.09 ± 0.16 , 1.03 ± 0.11 , 1.05 ± 0.09 , and 1.06 ± 0.09 , respectively. There was a strong correlation between the CT-DR $_{Ssc/Isp+TM}$ of the Y + 2.5 or Y + 5 sections and that of the entire muscle volume ($r = 0.825$ and 0.862 , respectively).

Table 1 summarizes the results of step A.

Step B

A total of 17 CT images of 17 patients were included in this study. The patients' clinical and morphological data are summarized in Table 2. Interobserver reproducibility was good for all 3D volumes, with a mean ICC value of 0.838.

The observed ratios of muscle volume (VR $_{Ssc/Isp+TM}$) for Y, Y + 2.5 and Y + 5 sections were 1.12 ± 0.55 , 1.21 ± 0.28 , and 1.13 ± 0.16 , respectively. The observed ratios of CT density (CT-DR $_{Ssc/Isp+TM}$) for Y, Y + 2.5 and Y + 5 sections were 1.02 ± 0.11 , 0.92 ± 0.07 , and 0.92 ± 0.05 , respectively.

Table 3 summarizes the results of step B.

	Y section	Y + 2.5 cm section	Y + 5 cm section	Whole muscle
Volume (ml)				
Ssc	24.9 ± 6.7	51.1 ± 9.8	71.7 ± 13.9	113.4 ± 26.2
Isp + TM	23.9 ± 7.3	48.1 ± 11.7	69.4 ± 17.0	107.7 ± 28.1
CT density (HU)				
Ssc	47.2 ± 6.2	49.2 ± 7.1	49.4 ± 7.5	48.6 ± 7.6
Isp + TM	44.8 ± 10.4	48.4 ± 9.8	47.6 ± 9.3	46.1 ± 8.9
Ratio of muscle volume and CT density				
VR $_{Ssc/Isp+TM}$ *	1.09 ± 0.27	1.09 ± 0.17	1.06 ± 0.16	1.06 ± 0.10
P corr	0.480	0.651	0.566	
CT-DR $_{Ssc/Isp+TM}$ *	1.09 ± 0.16	1.03 ± 0.11	1.05 ± 0.09	1.06 ± 0.09
P corr	0.588	0.825	0.862	

Table 1. Observed sectional ratios of muscle volume and CT density for patients with clavicular fracture (step A). Data are presented as means \pm standard deviations. Sectional measurement of each shoulder muscle is performed as follows: from the most lateral end of the muscles to the plane of Y-view (Y section), to the plane 2.5 cm medial to the Y-view (Y + 2.5 cm section), and to the plane 5 cm medial to the Y-view (Y + 5 cm section). CT-DR CT density ratio, HU hounsfield unit, Isp infraspinatus, P corr, pearson's correlations, Ssc subscapular, TM teres minor, VR volume ratio. *VR $_{Ssc/Isp+TM}$ = ratio of the muscle volume between the subscapularis and infraspinatus or teres minor. CT-DR $_{Ssc/Isp+TM}$ = ratio of CT density between the subscapularis and infraspinatus or teres minor. For each section, the Pearson's correlations (P corr) between the whole muscle and each section of the data are calculated.

Variable	Value
Age, years, mean \pm SD	26.5 \pm 8.4
Sex, male	12 (71)
Side, right	7 (41)
Symptom duration, month, mean \pm SD	100 \pm 97
Symptomatic dislocation times, n (%)	
≥ 10	9 (53)
<10	8 (47)
Sports activity level, high/medium/low	6/0/11
Work level, high/medium/low	5/11/1
Preoperative range of motion, degree, mean \pm SD	
Forward flexion	158.7 \pm 31.0
Abduction	154.3 \pm 31.9
Preoperative morphological findings	
Glenoid rim morphology, normal/erosion/fragment	3/6/8
Erosion, none/small/large	11/3/3
Fragment, none/small/large	9/2/6
Hill-Sachs lesion, none/small/large	1/7/9
AIGHL hyperlaxity	10 (58)
Capsule tear	1 (6)

Table 2. Clinical and morphological data of patients with anterior shoulder instability (step B). Unless otherwise indicated, data are presented as number (%) of patients. AIGHL anterior inferior glenohumeral ligament, SD standard deviation.

	Y section	Y + 2.5 cm section	Y + 5 cm section
Volume (ml)			
Ssc	34.3 \pm 10.5	76.4 \pm 15.2	109.3 \pm 21.4
Isp + TM	34.9 \pm 11.2	65.8 \pm 16.1	97.9 \pm 19.1
CT density (HU)			
Ssc	59.9 \pm 6.2	59.5 \pm 5.1	59.4 \pm 4.6
Isp + TM	59.2 \pm 5.6	65.1 \pm 5.4	64.8 \pm 5.1
Ratio of muscle volume and CT density			
VR _{Ssc/Isp+TM} *	1.12 \pm 0.55	1.21 \pm 0.28	1.13 \pm 0.16
CT-DR _{Ssc/Isp+TM} *	1.02 \pm 0.11	0.92 \pm 0.07	0.92 \pm 0.05

Table 3. Observed sectional ratios of muscle volume and CT density for patients with anterior shoulder instability (step B). Data are presented as means \pm standard deviations. Sectional measurement of each shoulder muscle is performed as follows: from the most lateral end of the muscles to the plane of Y-view (Y section), to the plane 2.5 cm medial to the Y-view (Y + 2.5 cm section), and to the plane 5 cm medial to the Y-view (Y + 5 cm section). CT-DR CT density ratio, HU Hounsfield unit, Isp infraspinatus, Ssc subscapular, TM teres minor, VR volume ratio. *VR_{Ssc/Isp+TM} = ratio of the muscle volume between the subscapularis and infraspinatus or teres minor. CT-DR_{Ssc/Isp+TM} = ratio of CT density between the subscapularis and infraspinatus or teres minor.

Comparison and post hoc power analysis

All sectional muscle volume, CT density, and CT-DR_{Ssc/Isp+TM} data differed significantly between the CF (Step A) and ASI (Step B) groups. However, the differences in VR_{Ssc/Isp+TM} were unclear. Post hoc power analysis showed more variable estimated sample sizes for the muscle volume of Ssc and Isp + TM than for CT density. The estimated sample size for VR_{Ssc/Isp+TM} was considerably larger. Table 4 summarizes the results of the comparison and post hoc power analysis.

Discussion

In the present study, we observed that the ratios of shoulder muscle volume (VR_{Ssc/Isp+TM}) and CT density (CT-DR_{Ssc/Isp+TM}) were balanced in our patient cohort with CF. In addition, these ratios were constant to some extent, whether they were derived from the sectional or whole measurements. In patients with ASI, the VR_{Ssc/Isp+TM} was relatively high, whereas the CT-DR_{Ssc/Isp+TM} was relatively low, implying the possibility of an imbalance between the anterior and posterior shoulder muscles. For CT-DR_{Ssc/Isp+TM} a statistically significant intergroup difference

	<i>P</i> -value	Cohen's d value	Estimated size
Volume of Ssc			
Y section	<0.001	1.10	21
Y + 2.5 cm section	<0.001	2.04	7
Y + 5 cm section	<0.001	2.14	7
Volume of Isp + TM			
Y section	<0.001	1.20	18
Y + 2.5 cm section	<0.001	1.29	11
Y + 5 cm section	<0.001	1.56	11
CT density of Ssc			
Y section	<0.001	2.01	7
Y + 2.5 cm section	<0.001	1.57	11
Y + 5 cm section	<0.001	1.48	12
CT density of Isp + TM			
Y section	<0.001	1.57	8
Y + 2.5 cm section	<0.001	1.93	8
Y + 5 cm section	<0.001	2.11	7
VR _{Ssc/Isp+TM} *			
Y section	0.401	0.08	3973
Y + 2.5 cm section	0.047	0.53	86
Y + 5 cm section	0.076	0.45	118
CT-DR _{Ssc/Isp+TM} *			
Y section	0.067	-0.49	18
Y + 2.5 cm section	<0.001	-1.22	18
Y + 5 cm section	<0.001	-1.63	10

Table 4. Comparison and post hoc power analysis of patients with clavicular fracture (step A) versus anterior shoulder instability (step B). Student t-test was used to compare the Step A and B results. Furthermore, to determine the study's ability to detect a significant effect, a power analysis for the comparison was performed, and Cohen's d value and estimated sample size were obtained. Sectional measurement of each shoulder muscle were performed as follows: from the most lateral end of the muscles to the plane of Y-view (Y section), to the plane 2.5 cm medial to the Y-view (Y + 2.5 cm section), and to the plane 5 cm medial to the Y-view (Y + 5 cm section). *CT-DR* CT density ratio, *Isp* infraspinatus, *Ssc* subscapular, *TM* teres minor, *VR* volume ratio. *VR_{Ssc/Isp+TM} = ratio of muscle volume between the subscapularis and infraspinatus or teres minor; CT-DR_{Ssc/Isp+TM} = ratio of CT density between the subscapularis and infraspinatus or teres minor.

was noted and the sample size was sufficient to account for the statistical significance. This was not the case for VR_{Ssc/Isp+TM}.

Considering the balance of the antagonistic muscles is crucial because they may be associated with the causes and consequences of articular diseases. The balance of the shoulder muscles in the transverse force couple has been debated. Espinosa-Uribe et al. conducted a study on 304 shoulders from 152 patients of different ages and sexes and observed a ratio of the rotator cuff transverse force couple volume (corresponding to VR_{Ssc/Isp+TM}) of 1.02 ± 0.18 without significant differences across all ages and sexes⁹. Piepers et al. reported similar results in non-pathologic shoulders, demonstrating that the muscle volume of the transverse force couple was kept balanced¹⁴. In our study, we confirmed a VR_{Ssc/Isp+TM} of 1.06 ± 0.10 in the CF group (non-pathologic shoulder), which was consistent with the previous results^{9,14}.

Our study also suggested that the CT density ratio in the shoulder muscle transverse force couple (CT-DR_{Ssc/Isp+TM}) was almost balanced. In similar studies focusing on the osteoarticular areas, both muscle volume and CT density could be used as an indicator of the muscle atrophy and degeneration. For instance, the CT density of the gluteus medius muscle reflects muscle strength in patients with hip osteoarthritis¹⁵. In the shoulder area, van de Sande et al. examined shoulder CT from patients with rheumatoid arthritis and observed a strongly correlation between the CT density of the rotator cuff muscle volume and visual assessment of fatty degeneration¹⁶. However, no study specifically investigated the CT-DR_{Ssc/Isp+TM} in pathologic or non-pathologic shoulder. In this regard, our study was the first to show that CT-DR_{Ssc/Isp+TM} was balanced in non-pathological shoulders, indicating that the internal properties of muscles and their volumes might be balanced in the shoulder muscle transverse force couple.

Although the measurement of muscle density has been recognized as a feasible method for observing muscle degeneration, studies utilizing this approach are limited because exposure to radiation poses an inevitable problem for CT. In contrast, quantitative assessments of muscle degeneration using MRI, such as the fat fraction ratio, have been more widely used. In fact, CT is primarily used for the confirmation of fractures or other bone abnormalities; hence, they are more limited than MRI. Moreover, CT can be used to assess shoulder instability,

but it is not the primary diagnostic tool. Therefore, we believe that MRI will be required in the future since it is more useful for this indication than current methods.

In this study, we evaluated the feasibility of VR_{Ssc/Isp+TM} and CT-DR_{Ssc/Isp+TM} derived from sectional muscle measurements. Sectional muscle assessment offered advantages in cases where the shoulder muscles were only partially imaged. It provided valuable information for evaluating morphological changes and the degree of medial retraction of the rotator cuff muscles. A recent study by Chung et al. described that 3D sectional volume analysis of the supraspinatus muscle can be useful for evaluating accurate serial changes of muscle atrophy after arthroscopic repair surgery of rotator cuff tears¹³. Although their research was noteworthy, one of the limitations was that they were unable to measure the entire supraspinatus muscle because of the practical difficulty in extending the field of the shoulder MRI. Thus, our study was the first to compare sectional muscle data with the whole muscle data in non-pathological shoulders. We observed a mild to moderate correlation between the VR_{Ssc/Isp+TM} for each section and that for the total muscle. Conversely, the CT-DR_{Ssc/Isp+TM} for each section and the whole also did not significantly differ, and a strong correlation was observed between the CT-DR_{Ssc/Isp+TM} of Y + 2.5 cm or Y + 5 cm section and that of the total volume. This indicated that the muscle volume may be easily affected by factors, such as a slight difference in scan positioning, and is expected to be more susceptible to sectional evaluation. Muscle CT density, in contrast, would be less influenced by these factors and could be a more favorable parameter for evaluating muscle properties in a sectional manner.

In our study, we applied our sectional evaluation system of VR_{Ssc/Isp+TM} and CT-DR_{Ssc/Isp+TM} to ASI cases. Mitterer et al. recently evaluated VR_{Ssc/Isp+TM} in patients with posterior humeral head subluxation⁸ obtaining a value of 1.14 ± 0.13 using the total muscle volume. An attempt to measure the sectional muscle volume and CT density in patients with ASI has not been previously performed. Therefore, our study was the first to analyze these parameters in the ASI and compare them with the whole muscle data. In our analysis, the observed VR_{Ssc/Isp+TM} was 1.21 ± 0.28 and 1.13 ± 0.16 , whereas CT-DR_{Ssc/Isp+TM} was 0.92 ± 0.07 and 0.92 ± 0.05 for Y + 2.5 and Y + 5 sections, respectively. The VR_{Ssc/Isp+TM} ratios appeared to be higher than those of the non-pathologic shoulders, indicating hypertrophy of the anterior muscle (Ssc) and atrophy of the posterior muscle (Isp + TM). However, a comparatively lower CT-DR_{Ssc/Isp+TM} in the anterior muscle (Ssc) was associated with fatty degeneration, leading to a discrepancy of our findings. In a previous study on posterior humeral head subluxation⁸, the posterior driving force was assumed to be created by a larger anterior muscle (Ssc). In this case, we observed that the anterior muscle (Ssc) underwent mild atrophy and degeneration, while, the comparatively larger posterior muscle (Isp + TM) generated an anterior directional force; hence, repeated anterior-dominant dislocation occurred. This hypothesis does not explain the large sectional volume of the anterior muscle (Ssc).

Finally, in the present study, a statistically significant intergroup difference was observed in CT-DR_{Ssc/Isp+TM} but not in VR_{Ssc/Isp+TM}. Furthermore, post hoc power analysis showed variable effect sizes for muscle volume, whereas those for CT density were relatively stable. This may originate from the variability in the muscle volumes of Ssc and Isp + TM, as indicated by the large standard deviations across all sectional volumes. As stated above, compared with muscle CT density, muscle volume may be more influenced by factors such as scan positioning and sectional variation and is likely sensitive to sectional measurements. In contrast, CT is thought to be less sensitive to these factors, resulting in less variable results and more stable effect sizes. Therefore, CT-DR_{Ssc/Isp+TM} may be a reproducible and useful measurement tool for assessing muscle imbalance.

However, post hoc power calculations may pose a potential risk of misinterpretation. Because post hoc analysis tends to be applied especially when research findings are negative ($p \geq 0.05$), this will produce a low post hoc power result¹⁷. In general, several possibilities should be considered when interpreting such negative results: (1) there is a true association, but with a smaller effect size than expected, which could not be detected with the given sample size; (2) there is a true association with an effect larger than hypothesized, but it was not detected by chance; (3) the variance of the sample is greater than expected, so excessive noise in the data prevented the detection of a true association; and (4) confounding factors were unaccounted for, so the results appear as if there was no association¹⁸. These are all type II errors and should be considered when interpreting the negative results of our study (i.e., Ssc and Isp + TM muscle volumes and VR_{Ssc/Isp+TM}). Therefore, future studies would ideally require accurate pre-study power analyses and a careful study design.

Furthermore, it should be considered that CF is not an ideal control group for ASI since it represents a completely different background, especially in terms of age; as patients with CF were older than those with ASI, the differences in age may have influenced the results. On the other hand, these ratios were almost constant across ages and sexes; thus, the influence caused by differences in age could be minimal. To validate this finding, an age- and sex-matched control group must be considered in the future.

This study had several other limitations. First, although the muscle imbalance could be associated with shoulder instability, the instability is primarily related to the static structures such as labrum, capsule, ligaments, and bone. Since these structures were not addressed in the present study, they must be examined in a future analysis. Second, MRI is more frequently used as a diagnostic tool for shoulder instability than CT; thus, the implications of using CT in this study may be relatively limited. Therefore, it would be beneficial to develop an MRI-based assessment in the future. Third, the sample size was small, and the distribution of our cohort was unequal. Fourth, the absence of a true control group for ASI was another limitation because we had to select non-pathological shoulders with CF in this study, whose age and sex were different from those of the ASI cohort. Furthermore, we could not evaluate the entire muscle in the ASI cases. These issues should be addressed in future studies. Simultaneously, we tested the hypothesis that mild fatty degeneration occurs in the anterior muscles (Ssc). Another quantitative method, such as the MRI Dixon-based fat fraction ratio, should be introduced to resolve this issue.

Conclusion

Our study demonstrated that the ratio of volume (VR_{Ssc/Isp+TM}) and CT density (CT-DR_{Ssc/Isp+TM}) in the transverse force couple of shoulder muscles was balanced in non-pathologic shoulders with CF. Additionally, these ratios remained constant, regardless of whether they were derived from sectional or the whole muscle measurements. Furthermore, for ASI, VR_{Ssc/Isp+TM} was relatively high, whereas CT-DR_{Ssc/Isp+TM} was relatively low compared with those of the non-pathological shoulder. This suggested an imbalance between the anterior (Ssc) and posterior (Isp + TM) muscles of the shoulder.

Data availability

The authors declare that all the data supporting the findings of this study are available within the article.

Received: 23 February 2024; Accepted: 6 November 2024

Published online: 10 November 2024

References

1. Hurley, E. T. et al. Arthroscopic bankart repair versus conservative management for first-time traumatic anterior shoulder instability: a systematic review and meta-analysis. *Arthroscopy* **36**, 2526–2532. <https://doi.org/10.1016/j.arthro.2020.04.046> (2020).
2. Longo, U. G. et al. Multidirectional instability of the shoulder: a systematic review. *Arthroscopy* **31**, 2431–2443. <https://doi.org/10.1016/j.arthro.2015.06.006> (2015).
3. Blonna, D. et al. Arthroscopic bankart repair versus open Bristow-Latarjet for shoulder instability: a matched-pair multicenter study focused on return to sport. *Am. J. Sports Med.* **44**, 3198–3205. <https://doi.org/10.1177/0363546516658037> (2016).
4. Heinsberg, L. W. & Weeks, D. E. Post hoc power is not informative. *Genet. Epidemiol.* **46** (7), 390–394. <https://doi.org/10.1002/gepi.22464> (2022).
5. Goutallier, D., Postel, J. M., Bernageau, J., Lavau, L. & Voisin, M. C. Fatty muscle degeneration in cuff ruptures. Pre- and postoperative evaluation by CT scan. *Clin. Orthop. Relat. Res.* **304**, 78–83 (1994).
6. Nakagawa, S. et al. Bipolar bone loss in male athletes with traumatic anterior shoulder instability: an evaluation using a new scoring system. *Orthop. J. Sports Med.* **6**, 2325967118782420. <https://doi.org/10.1177/2325967118782420> (2018).
7. Şahin, K., Kendirci, A. Ş., Albayrak, M. O., Sayer, G. & Erşen, A. Multidirectional instability of the shoulder: surgical techniques and clinical outcome. *EFORT Open. Rev.* **7**, 772–781. <https://doi.org/10.1530/EOR-22-0010> (2022).
8. Liavaag, S. et al. Immobilization in external rotation after primary shoulder dislocation did not reduce the risk of recurrence: a randomized controlled trial. *J. Bone Joint Surg. Am.* **93**, 897–904. <https://doi.org/10.2106/JBJS.J.00416> (2011).
9. Espinosa-Uribe, A. G. et al. An age- and gender-related three-dimensional analysis of rotator cuff transverse force couple volume ratio in 304 shoulders. *Surg. Radiol. Anat.* **39**, 127–134. <https://doi.org/10.1007/s00276-016-1714-x> (2017).
10. Levine, M. & Ensom, M. H. Post hoc power analysis: an idea whose time has passed? *Pharmacotherapy* **21** (4), 405–409. <https://doi.org/10.1592/phco.21.5.405.34503> (2001).
11. Momose, T. et al. CT-based analysis of muscle volume and degeneration of gluteus medius in patients with unilateral hip osteoarthritis. *BMC Musculoskelet. Disord.* **18**, 457. <https://doi.org/10.1186/s12891-017-1828-2> (2017).
12. Thomazeau, H., Boukobza, E., Morcret, N., Chaperon, J. & Langlais, F. Prediction of rotator cuff repair results by magnetic resonance imaging. *Clin. Orthop. Relat. Res.* **344**, 275–283. <https://doi.org/10.1097/00003086-199711000-00027> (1997).
13. Chung, S. W. et al. Serial changes in 3-dimensional supraspinatus muscle volume after rotator cuff repair. *Am. J. Sports Med.* **45**, 2345–2354. <https://doi.org/10.1177/0363546517706699> (2017).
14. Mohtadi, N. G. et al. A randomized clinical trial comparing open and arthroscopic stabilization for recurrent traumatic anterior shoulder instability: two-year follow-up with disease-specific quality-of-life outcomes. *J. Bone Joint Surg. Am.* **96**, 353–360. <https://doi.org/10.2106/JBJS.L.01656> (2014).
15. Mitterer, M., Matis, N., Steiner, G., Vasvary, I. & Ortmaier, R. Muscle volume imbalance may be associated with static posterior humeral head subluxation. *BMC Musculoskelet. Disord.* **22**, 279. <https://doi.org/10.1186/s12891-021-04146-3> (2021).
16. Piepers, I., Boudt, P., Van Tongel, A. & De Wilde, L. Evaluation of the muscle volumes of the transverse rotator cuff force couple in nonpathologic shoulders. *J. Shoulder Elb. Surg.* **23**, e158–e162. <https://doi.org/10.1016/j.jse.2013.09.027> (2014).
17. van de Sande, M. A., Stoele, B. C., Obermann, W. R., Tjong a Lieng, J. G. & Rozing, P. M. Quantitative assessment of fatty degeneration in rotator cuff muscles determined with computed tomography. *Invest. Radiol.* **40**, 313–319. <https://doi.org/10.1097/01.rli.000016014.16577.86> (2005).
18. Zanetti, M., Gerber, C. & Hodler, J. Quantitative assessment of the muscles of the rotator cuff with magnetic resonance imaging. *Invest. Radiol.* **33**, 163–170. <https://doi.org/10.1097/00004424-199803000-00006> (1998).

Author contributions

Substantial contributions to the conception: KN, YH and MN. Design of the work: KN, YH and MN. Patient acquisition: KS. Data analysis: KN, YH, HS, KM, KI and MN. Data interpretation: KN, YH, HS, KM, KI and MN. Drafted the work: KN, HS and EK. Substantively revised: KN, KS and MN.

Declarations

Competing interests

The authors declare no competing interests.

Additional information

Supplementary Information The online version contains supplementary material available at <https://doi.org/10.1038/s41598-024-79065-z>.

Correspondence and requests for materials should be addressed to K.N.

Reprints and permissions information is available at www.nature.com/reprints.

Publisher's note Springer Nature remains neutral with regard to jurisdictional claims in published maps and institutional affiliations.

Open Access This article is licensed under a Creative Commons Attribution-NonCommercial-NoDerivatives 4.0 International License, which permits any non-commercial use, sharing, distribution and reproduction in any medium or format, as long as you give appropriate credit to the original author(s) and the source, provide a link to the Creative Commons licence, and indicate if you modified the licensed material. You do not have permission under this licence to share adapted material derived from this article or parts of it. The images or other third party material in this article are included in the article's Creative Commons licence, unless indicated otherwise in a credit line to the material. If material is not included in the article's Creative Commons licence and your intended use is not permitted by statutory regulation or exceeds the permitted use, you will need to obtain permission directly from the copyright holder. To view a copy of this licence, visit <http://creativecommons.org/licenses/by-nc-nd/4.0/>.

© The Author(s) 2024